

1/93

# ERRATA for Statistical Spectral Analysis

p. 8

$x(t)$  satisfies

$$x(t - v) = cx(t) \quad (7)$$

for all  $t$  if and only if

$$x(t) = Xe^{i2\pi ft} \quad (8)$$

complex  $X$   
and real  $f$

for some ~~real values of  $X$  and  $f$~~  (exercise 3). As a consequence, the form of a bounded function  $x(t)$  is invariant to convolution if and only if  $x(t) = Xe^{i2\pi ft}$ , in

p. 33

As a final item in this brief review it is pointed out that inspection of (13) and (32) reveals that if a function, say  $y$ , is given by the convolution of two other functions, say  $x$  and  $h$ , then the Fourier transform of  $y$ ,  $Y$ , is given by the product of Fourier transforms of  $x$  and  $h$ :  $Y = XH$ . This result is known as the *convolution theorem*. Additional review material is incorporated in exercises 2, 4, 7, 8, 9, 10, 12, 13, 14, and 16.

p. 42

twice

function  $A_{1/T}$ ). It is therefore of interest to determine the particular data-tapering window  $a_T$  of a given width that yields the finest possible spectral resolution. By adopting the square root of the second central moment (standard deviation) of the square of a function as a particular measure of its width, it can be shown [Franks 1969] that the product of widths of temporal and spectral apertures is minimized by the Gaussian aperture,

$$a_T(t) = \exp \left[ \frac{-(t/T)^2}{2} \right], \quad (16a)$$

The minimized resolution product is

$$\min\{\Delta r^\circ \Delta f^\circ\} = \frac{2}{\pi}, \quad \frac{2}{\pi} \quad (17)$$

twice the standard  
deviations

large

for which  $\Delta r^\circ$  and  $\Delta f^\circ$  are defined to be the ~~second central moments~~ of the (unsquared but positive) apertures, (16). Apertures that are more convenient for implementation such as (13) (and other measures of width) yield resolution products that are ~~closer to unity~~ than (17).

The general relation (10) and the specific bound (17) are referred to as

P. 51

$$\tau = 0, \pm T_s, \pm 2T_s, \dots, \pm T. \quad (67)$$

which is precisely the discrete-time counterpart of the continuous-time correlogram (19) (with the change of variables  $v = u \sqrt{|\tau|/2}$ ). The relation (64) can be shown to be a direct consequence of the convolution theorem for the FST

P. 60

21. Verify that the inverse FST is given by

$$x(t) = \int_{-1/2T_s}^{1/2T_s} \bar{X}(f) e^{i2\pi ft} df. \quad (109)$$

Nonstatistical Spectral Analysis Chap. 2

60

P. 61

where the FST is defined by (using  $T_s = 1$ )

$$\bar{X}(f) \triangleq \sum_{n=-\infty}^{\infty} x(n) e^{-i2\pi fn}. \quad (110)$$

Hint: Substitute (110) into (109) and use the identity

$$T_s \int_{-1/2T_s}^{1/2T_s} e^{i2\pi f n T_s} df = \begin{cases} 1, & n = 0 \\ 0, & n = \text{integer} \neq 0. \end{cases} \quad (111)$$

22. (a) Consider the sum of two sine waves as in exercise 3, and assume that the two

P. 97

17. Derive (7) in Appendix 3-2 from (4) and (5) in Appendix 3-2. Hint: See the note in exercise 9(a) in Chapter 4 regarding changes of variables in double integrals in order to reexpress (4)–(5) as

$$y(t) = \int_{-T}^T \hat{R}_s(\tau) R_{\tau}(t, \tau) d\tau.$$

P. 126

$$m(t, \tau) = g_{\Delta f}\left(t + \frac{\tau}{2}\right) a_{1/\Delta f}\left(\frac{\tau}{2}\right) \quad (79a)$$

$$\cong g_{\Delta f}(t) h_{1/\Delta f}(\tau), \quad \Delta t \Delta f \gg 1. \quad (79b)$$

Substitution of (79a) into (74) and then (74) into (73) yields (exercise 10)

$$y_f(t) = \{x(t)[x(t) \otimes (a_{1/\Delta f}(t) e^{i2\pi f t})]\} \otimes g_{\Delta f}(t). \quad (80)$$

p. 133

$$a' = \min s(u, v)$$

$$u \in [a, b]$$

$$v \in [c, d]$$

$$b' = \max s(u, v)$$

$$u \in [a, b]$$

$$v \in [c, d]$$

and then solve for  $c'$  and  $d'$  as functions of  $\tau$ , using the same minimization and maximization methods on  $r[u, v]$  but subject to the constraint  $s(u, v) = \tau$  for each  $\tau \in [a', b']$ . As an exercise, show that for  $a = c$ ,  $b = d$ ,  $t = (u + v)/2$ ,  $\tau = v - u$ , we obtain  $J = 1$ ,  $a'' = c - \tau/2$ ,  $b'' = d - \tau/2$ ,  $c' = c + \tau/2$ ,  $d' = d + \tau/2$ . Hint: Draw a picture that describes this change of variables as a transformation of coordinates in a plane and shows the region of integration as a rectangle.

(b) Consider the quadratic time-invariant transformation

p. 159

where  $\delta_{f-\alpha}$  is the Kronecker delta, and the temporal variance is given by (exercise

1)

$$\text{var}\{\bar{X}_T(t, f)\} = \hat{S}_a(f) \otimes z_{1/T}(f) + \sum_{\alpha} |m_{\alpha}|^2 \left[ \frac{1}{T} w_{1/T}(f - \alpha) - \delta_{f-\alpha} \right]^2. \quad (87)$$

Thus, as the length  $T$  of the data segment is increased, the coefficient of variation

p. 161

Rectangle (Dirichlet):

$$h(\tau) = \begin{cases} 1, & |\tau| \leq T/2 \\ 0, & |\tau| > T/2 \end{cases} \quad (91a)$$

Triangle (Bartlett or Fejér):

$$h(\tau) = \begin{cases} 1 - \frac{2|\tau|}{T}, & |\tau| \leq T/2 \\ 0, & |\tau| > T/2 \end{cases} \quad (92a)$$

Raised Cosine (von Hann):

$$h(\tau) = \begin{cases} \frac{1}{2} \left[ 1 + \cos\left(\frac{2\pi\tau}{T}\right) \right], & |\tau| \leq T/2 \\ 0, & |\tau| > T/2 \end{cases} \quad (93a)$$

Raised Cosine on a Platform (Hamming):

$$h(\tau) = \begin{cases} 0.54 + 0.46 \cos\left(\frac{2\pi\tau}{T}\right), & |\tau| \leq T/2 \\ 0, & |\tau| > T/2 \end{cases} \quad (94a)$$

replace  
all  $T$ s  
with  $W$ s.

W

W

p. 162

Replace all  
T with W

Blackman:

$$h(\tau) = \begin{cases} 0.42 + 0.50 \cos\left(\frac{2\pi\tau}{T}\right) + 0.08 \cos\left(\frac{4\pi\tau}{T}\right), & |\tau| \leq T/2 \\ 0, & |\tau| > T/2. \end{cases} \quad (95a)$$

These windows are identical for discrete and continuous time. The corresponding Fourier-series transforms (using the sampling increment  $T_s = 1$ ) are as follows:

Dirichlet (Rectangle):

$$H(f) = \frac{\sin(\pi f T)}{\sin(\pi f)}, \quad |f| \leq \frac{1}{2} \quad (91b)$$

Bartlett or Fejér (Triangle):

$$H(f) = \frac{2}{T} \left[ \frac{\sin(\pi f T/2)}{\sin(\pi f)} \right]^2, \quad |f| \leq \frac{1}{2} \quad (92b)$$

von Hann (Raised Cosine):

$$H(f) = \frac{1}{2} \frac{\sin(\pi f T)}{\sin(\pi f)} + \frac{1}{4} \frac{\sin \pi(f - 1/T)}{\sin \pi(f - 1/T)} + \frac{1}{4} \frac{\sin \pi(f + 1/T)}{\sin \pi(f + 1/T)}, \quad |f| \leq \frac{1}{2} \quad (93b)$$

Hamming (Raised Cosine on a Platform):

$$H(f) = 0.54 \frac{\sin(\pi f T)}{\sin \pi f} + 0.23 \frac{\sin \pi(f - 1/T)}{\sin \pi(f - 1/T)} + 0.23 \frac{\sin \pi(f + 1/T)}{\sin \pi(f + 1/T)}, \quad |f| \leq \frac{1}{2} \quad (94b)$$

Blackman:

$$H(f) = 0.42 \frac{\sin(\pi f T)}{\sin(\pi f)} + 0.25 \frac{\sin \pi(f - 1/T)}{\sin \pi(f - 1/T)} + 0.25 \frac{\sin \pi(f + 1/T)}{\sin \pi(f + 1/T)} + 0.04 \frac{\sin[(\pi/2)(f + 2/T)]}{\sin \pi(f + 2/T)} + 0.04 \frac{\sin[(\pi/2)(f - 2/T)]}{\sin \pi(f - 2/T)}, \quad |f| \leq \frac{1}{2}. \quad (95b)$$

For  $T \gg 1$ , these spectral windows are essentially the same as the Fourier transforms of the continuous-time counterparts for  $|f| \leq 1/2$ .

In addition to these five spectral windows, there is the rectangle spectral window,

$$H(f) = \begin{cases} 1, & |f| \leq 1/2 \\ 0, & |f| > 1/2, \end{cases} \quad (96)$$

which is referred to as the *Daniell window*. The four spectral windows (91b)-(94b) are shown in Figure 5-5. Observe how much smaller the sidelobes are for the second two compared with the first two. The Hamming window is designed

p. 163

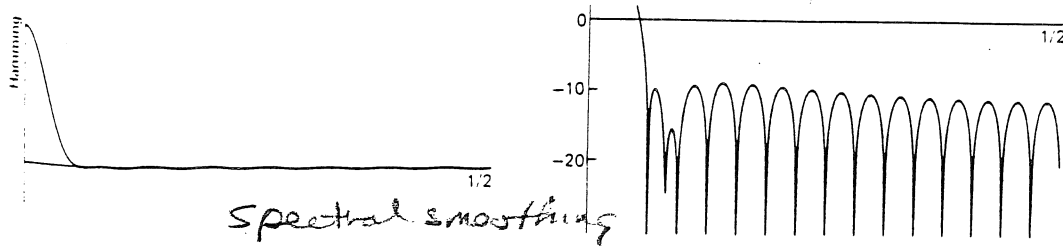


Figure 5-5 ~~Correlation tapering~~ windows (left) displayed with linear ordinate and ~~spectral smoothing~~ windows (right) displayed with log ordinate (from (91)–(95) with  $T = 32$ ).

Sec. D Resolution, Leakage, and Reliability: Design Trade-Offs

163

p. 164

TABLE 5-2 SPECTRAL WINDOW PARAMETERS

Effective spectral window	Highest sidelobe (dB)	Asymptotic decay rate (dB/octave)	3-dB bandwidth ( $\times T$ )	Reliability factor $\eta_0$
Dirichlet (rectangle)	-6.5	-3	1.21	1

p. 164

3-dB bandwidth of the main lobe, and the reliability factor

(with  $W=T$ )

$$\eta_0 = \frac{\sum h_i^2(\tau)}{T h_1^2(0)} \quad (97)$$

which occurs in the discrete-time counterpart to the proportionality coefficient  $\eta$  (75) that determines the coefficient of variation (77). The factor  $\eta_0$  in (97) depends not only on the particular window but also on the number of time samples per window width  $T$ ; however, this latter dependence becomes negligible as the number of time-samples increases ( $T \gg 1$ ). Therefore, the values given in Table 5-2 are asymptotic values for (97) obtained from the continuous-time counterparts of the windows.<sup>5</sup> Observe that if the temporal windows in Table 5-2, (91a)–(95a), are data-tapering windows rather than effective autocorrelation-tapering windows, then  $|H(f)|^2$  rather than  $H(f)$  is the effective spectral smoothing window for a temporally smoothed periodogram, and therefore the decibel values

and  $\Delta f = 1/W$

<sup>5</sup> Since  $\Delta f/\eta_0$  in (77) with  $\eta = \eta_0$  can be interpreted as an effective bandwidth, then  $1/\eta_0$  is sometimes called the *standardized bandwidth* but should not be confused with the resolution bandwidth (e.g., the 3-dB bandwidth in Table 5-2).

$$\gamma_{ff} \approx \frac{\eta}{\Delta t \Delta f}$$

p. 165

for frequencies sufficiently far removed from zero ( $|f| > 1/T$ ). For a time-averaged periodogram, the factor  $\eta$  in (98), which is defined by (75), reduces to the reliability factor

$$\eta = \frac{\Delta f \int_{-\infty}^{\infty} h_T^2(\tau) d\tau}{h_T^2(0)} \approx \Delta f W \eta_0 \quad (99)$$

p. 166

where  $a_T(\tau)$  is the data-tapering window. It follows from (98) and (99) that for a coefficient of variation of  $1/b$ , we need a data segment of length

$$\Delta t = 10 \eta_1 T. \quad \text{with } W = 2T \quad (101)$$

For example, it follows from (100) and Table 5-2 that for no data tapering ( $a_T = \text{rectangle} \Rightarrow h_T = \text{triangle}$ ), the 3-dB resolution bandwidth is  $\Delta f = 1.78$  and the reliability factor is  $\eta_0 = 0.333$ , and therefore (101) becomes

$$\eta = \frac{W}{T} \eta_0 = 0.666$$

$$0.666 \quad \Delta t = \frac{(10)(0.333)(1.78)}{2 \Delta f_{3dB}} = \frac{5.9}{\Delta f_{3dB}}$$

3dB

Thus, for  $\Delta f = B/5$  and  $B = 1$  KHz, we need  $\Delta t \approx 30$  ms of data. For comparison, if we use a data-tapering window that yields an effective autocorrelation tapering window (100) that is the raised cosine (namely, the inverse transform of the square root of the magnitude of the transform of the raised cosine) to obtain better leakage behavior at the cost of moderately larger resolution bandwidth ( $\Delta f = 2/T$ ) and moderately larger reliability factor  $\eta_0 = 0.375$ , then (101) becomes

$$(\eta = \frac{W}{T} \eta_0 = 0.75)$$

$$0.75 \quad \Delta t = \frac{(10)(0.375)(2)}{2 \Delta f_{3dB}} = \frac{7.5}{\Delta f_{3dB}}$$

using  $W = 2T$

and therefore we need  $\Delta t = 37.5$  ms of data. This is only a 25% increase, but it

p. 166

3dB

As another alternative, a spectrally smoothed periodogram with the rectangle smoothing window can be used. Then since  $\Delta t \Delta f \gg 1$ , approximation (54b) can be used for the effective spectral window to obtain the approximate 3-dB bandwidth ( $\Delta f = 1/T$ ) and approximate reliability factor ( $\eta_f = 1$ ); however, the exact formula (54a) must be used to determine the sidelobe behavior. For example, with no data tapering, the asymptotic decay rate will be that of the Fejér spectral window, which is the same as it was for the time-averaged periodogram with no data tapering. However, the highest sidelobe will be lower (and will continually decrease as  $\Delta t \Delta f$  is increased). The cost of this improvement is that  $\Delta t = 50$  ms of data is needed, which is an increase of 67% above the 30 ms needed for the time-averaged periodogram with no data tapering.

3dB

Observe that if the desired spectral resolution width were cut in half to  $\Delta f = B/10$ , then for the same coefficient of variation, the amount of data required is simply doubled in each of the cases considered.

p. 177

3dB

of  $\Delta f = B/5$ , when triangle data tapering is used. Compare the result with the results in the example.

(with  $T = W/4$ )

- (d) Consider the second example in Section D, and evaluate the fractional leakage at  $f = f_0$  for triangle data tapering, when the sine wave frequency is  $f_* = f_0 + B/5, f_0 + 3B/10, f_0 + 2B/5$ , and the sine wave power is  $P_* = 2B|K(f_0)|^2$ . Explain any unexpected results and discuss practical implications.

15. Consider the problem of designing a wave analyzer using conventional analog electrical circuitry, that is, passive resistive-inductive-capacitive networks. The simplest BPF to implement would be a second-order resonant circuit with impulse-response function

$$k(t) = e^{-t/T} \cos(2\pi f t), \quad t \geq 0,$$

and the simplest LPF to implement would be the first-order circuit with impulse response function

$$g(t) = e^{-t/T}, \quad t \geq 0.$$

Determine the following characteristics of this spectrum analyzer:

- (a) Effective data-tapering window.
- (b) Effective autocorrelation-tapering window.
- (c) Effective spectral smoothing window and its 3-dB bandwidth ( $E(\Delta f/2) = E(0)/2$ ). 3dB
- (d) Time-averaging window.
- (e) Reliability factor (75).
- (f) Highest sidelobe (if any) of the effective spectral smoothing window.
- (g) Rate of decay of spectral window sidelobes (skirts).

Hint: Use the fact established in Chapter 4, Section E, that the real implementation described here is essentially equivalent to the complex implementation with BPF

$$k(t) = e^{-t/T} e^{j2\pi f t}.$$

provided that  $\Delta t/T \gg 1$  and  $|f|T \gg 1$ .

16. Consider the problem of designing a swept-frequency wave analyzer for audio spectral analysis. Assume that the spectral band to be analyzed ranges from 300 Hz to 15,000 Hz, the desired resolution is 100 Hz, and the desired coefficient of variation is  $1/10$ . Also assume that at each frequency  $f$  in the band that is swept across, one can treat the swept frequency analyzer as an unswept wave analyzer with the particular filters described in exercise 15. In order to specify design parameters for this spectrum analyzer, determine the following characteristics:

- (a) The time constant  $T$  required for a 3-dB resolution bandwidth of  $\Delta f = 100$  Hz. 3dB
- (b) The time constant  $\Delta t$  required for a coefficient of variation of  $1/10$ . 3dB
- (c) The sweep rate  $\beta = \Delta f / \Delta t$ . 3dB
- (d) The analysis time  $AT$  ( $AT$  = period of sweep).
- (e) If it is desired to detect a very brief audio event that occupies a band of width 500 Hz, what is the fraction-of-time probability of detection using this spectrum analyzer?
- (f) Assume that there is a constraint to cut the analysis time to half that found in (d). Propose a modification to the above design to meet this constraint; that is, adjust the requirements on sweep rate, resolution, and reliability.

Answers: (a)  $T = 1/100\pi$  s. (b)  $\Delta t = 5/100\pi$  s. (c)  $\beta = 2000\pi$  Hz/s. (d)  $AT = 7.35/\pi$  s. (e) Probability = 0.034. (f) Since  $\beta$  must be doubled and since  $\Delta t \Delta f = (\Delta f)^2 / \beta$ , then if reliability is held fixed  $\Delta f$  must be increased by the factor  $\sqrt{2}$ , or if  $\Delta f$  is held fixed then the coefficient of variation is doubled.

17. Evaluate the coefficient of variation  $R(f)$  given by (73) for the spectrum estimates specified in exercise 9(a)–(g).

p. 176

14. Consider the hopped time-averaged periodogram of triangle-tapered data as a statistical spectrum.

- (a) Determine the 3-dB bandwidth of the  $\text{sinc}^4$  spectral window, which results from a triangle data-tapering window. That is, determine the value of  $f$  at which

$$\left[ \frac{\sin(\pi f T)}{\pi f T} \right]^4 = \frac{1}{2},$$

and then double this value of  $f$ . Compare the result with that for the triangle autocorrelation tapering window (which corresponds to no data tapering) from Table 5-2.  $W_{eff} = W = 2T$ .

- (b) Determine the reliability factor  $\eta_0$  (99) for the  $\text{sinc}^4$  spectral window, and compare the result with that for the triangle autocorrelation tapering window. *Hint:* The corresponding effective autocorrelation tapering window for  $\text{sinc}^4$  is  $w_{eff}$

$$h_{eff}(\tau) = T v_T(\tau) \otimes v_T(\tau), \quad W = 4T$$

where  $v_T(\tau)$  is the unit-area triangle window with base of width  $2T$ . Use this convolution characterization to show that

$$h_{eff}(\tau) = \begin{cases} 1 - \frac{3}{4} \left( \frac{\tau}{T} \right)^2 + \frac{3}{4} \left| \frac{\tau}{T} \right|^3, & |\tau| \leq T \\ 2 \left( 1 - \frac{1}{2} \left| \frac{\tau}{T} \right| \right)^3, & T \leq |\tau| \leq 2T \\ 0, & |\tau| > 2T. \end{cases}$$

2.54/W

- (c) Consider the first example in Section D, and use the results of (a) (3-dB bandwidth  $= 0.636/T$ ) and (b) ( $\eta_0 = 0.269$ ) to determine the length  $\Delta t$  of data segment needed for a coefficient of variation of  $r_{yy} = 1/10$  and a spectral resolution width

p. 198

5

optimizing this type of spectrum estimate in order to minimize spectral leakage is to optimize the band-pass filter for each value of  $f$  to minimize the average power  $\bar{y}_{x_{1/\Delta f}}(t, f)_{\Delta f}$  at its output subject to the constraint that the strength of its response to an input sine wave of frequency  $f$  is equal to unity,

$$\sum_{u=0}^{N-1} a_{1/\Delta f}^f(u) e^{i2\pi f(t-u)} = e^{i2\pi f t}. \quad (48)$$

p. 224

## 2. Fourier Transformation of Tapered Cross Correlation

11

By analogy with the argument in Chapter 4, Section B, it is easily shown (exercise 10) that the two spectrally smoothed statistical cross spectra, of which (8) and (10) are examples, can be obtained by Fourier transformation of tapered cross correlations,



p. 259

and corresponding impulse-response sequence denoted by  $g_n^{-1}$ . The white excitation of the inverse model

$$z_n = g_n^{-1} \otimes x_n(r) \quad (17a)$$

is called the *innovations representation* for  $x_n(r)$ ,

$$x_n(r) = g_n \otimes z_n. \quad (17b)$$

because each new value  $z_n$  of the time-series is uncorrelated with all prior values  $\{z_j : j < n\}$  of the time-series and therefore provides completely new information—an *innovation*. Since  $g_n$  is a causal stable sequence, then (17a) reveals that  $x_n(r)$

## Sec. B Autoregressive Modeling Theory

259

p. 260

also admits a stable MA model (see (87) in Chapter 3) with transfer function given by

$$\bar{G}(f) = \sum_{q=0}^{L-1} b_q (e^{-i2\pi f})^q \quad (18)$$

in which the order  $L$  is possibly infinite and  $b_q = g_q$ . It is easy to show that if  $L$  is finite, then  $M$  in (3) is infinite, and if  $M$  is finite, then  $L$  in (18) is infinite. Also, either model can be obtained from the other by polynomial division of its

p. 261

where  $f_{x(L)}[x_n(L)]$  is the  $L$ th-order joint fraction-of-time probability density for the vector of  $L$  variables  $\{x_{k+1}, x_{k+2}, \dots, x_{k+L}\}$ ,

$$f_{x(L)}(z) \triangleq \frac{\partial^L}{\partial z_1 \partial z_2 \dots \partial z_L} \lim_{K \rightarrow \infty} \frac{1}{K} \sum_{k=0}^{K-1} U[z_1 - x_{k+1}] U[z_2 - x_{k+2}] \dots U[z_L - x_{k+L}], \quad (21)$$

p. 330

replace brackets [ ] with vertical bars | |

corresponding to a causal time-invariant filter with discrete-impulse response sequence  $g_n$  and show that

$$\ln(|A|) = (L) \ln(g_0)$$

- (c) Use the results of (a) and (b) to show that the relative entropy rate (20) for the time-series defined by

$$y_n \triangleq [y_0, y_1, y_2, \dots, y_{n-1}]'$$

with  $n \rightarrow \infty$  is given by

$$\bar{H}_y = \bar{H}_x + \ln(g_0) \quad (159)$$

- (d) It can be shown [Doob 1953] that for a minimum-phase linear time-invariant transformation, with transfer function  $\bar{G}(f)$ , we have

$$\ln(g_0) = \int_{-1/2}^{1/2} \ln|\bar{G}(f)| df. \quad (160)$$

Use (159) and (160) to prove that

p. 368

with frequency  $\alpha$  (but containing no first-order periodicity). It can be shown (exercise 5) using (2) and (5) and Parseval's relation for Fourier transforms that the power in the generated spectral line is given by

$$P^\alpha \triangleq \frac{1}{2} |\hat{M}_y^\alpha|^2 = \frac{1}{2} \left| \int_{-\infty}^{\infty} \int_{-\infty}^{\infty} k(u, v) \hat{R}_x^\alpha(u - v) e^{-i\pi\alpha(u+v)} du dv \right|^2 \quad (42)$$

$$= \frac{1}{2} \left| \int_{-\infty}^{\infty} K\left(f + \frac{\alpha}{2}, f - \frac{\alpha}{2}\right) \hat{S}_x^\alpha(f) df \right|^2, \quad \alpha \neq 0,$$

p. 381

- Thus, the Fourier transform of  $\hat{R}_x(\tau)$  cannot exhibit a spectral line at  $f = \alpha$ . Use this fact to show that the spectral line at  $\alpha$  (and at  $-\alpha$ ) in  $\hat{S}_x(f)$  is given by (3).
- (b) Use (5b) and (2) (with  $x(t)$  replaced by  $y(t)$ ) to show that  $\hat{M}_y^\alpha \neq 0$  for some  $\alpha$  if and only if  $\hat{R}_x^\alpha(\tau) \neq 0$ .
- (c) To gain some insight into the type of time-series that can exhibit discontinuities in the limit cyclic autocorrelation, consider the infinitely long chirp signal

$$x(t) = \sin(\beta t^2).$$

Verify the identity

1/2

l.c. ital.

p. 382

- (b) Show that this optimum QTI transformation can be implemented as the product of two filtered waveforms (see Figure 10-2)

$$y(t) = [h(t) \otimes x(t)] [v(t) \otimes x(t)],$$

382

Introduction to Second-Order Periodicity Chap. 10

l.c. ital.

p. 404

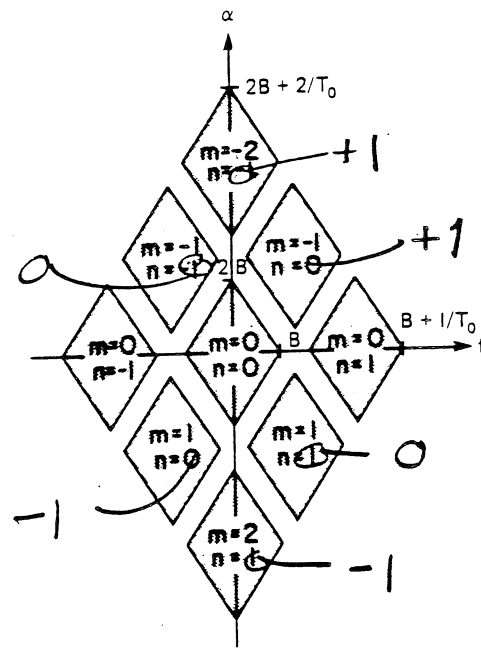


Figure 11-5 Regions of support of the spectral correlation function in the bi-frequency plane for a time-sampled bandlimited time-series.